Author Accepted Manuscript version of the paper by Ramon Abritta, Alexey Pavlov, Damiano Varagnolo, and Børre T. Børresen in the Proceedings of the ASME 2023 42nd OMAE, 8 (2023), DOI: https://doi.org/10.1115/OMAE2023-105003

Proceedings of the ASME 2023 42nd International Conference on Ocean, Offshore & Arctic Engineering
OMAE2023
June 11-16, 2023, Melbourne, Australia

OMAE2023-105003

PROBABILISTIC ECONOMIC ASSESSMENT OF AN OFFSHORE ENERGY HUB SUPPLYING ELECTRICAL POWER TO A FLOATING PRODUCTION STORAGE AND OFFLOADING UNIT

Ramon Abritta[1,*], Alexey Pavlov[1], Damiano Varagnolo[1], Børre T. Børresen[2]

[1]Norwegian University of Science and Technology, Trondheim, Norway
[2]Equinor ASA, Trondheim, Norway

ABSTRACT

This paper analyzes the viability of an offshore energy hub consisting of wind turbines, batteries, fuel cells and electrolyzers connected to, and powering, an oil producing floating production storage and offloading unit. We assess these components considering an oil production setup that strives for reduced CO_2 emissions. The problem is addressed from a probabilistic perspective. First, we utilize a quasirandom Monte Carlo approach to generate multiple scenarios regarding the uncertainties of the problem. Then, we evaluate the estimated net present value and total CO_2 emissions of the system. As a highlight, our method is capable of exploiting a larger variety of data and capturing more sources of uncertainties compared to the literature. Open-source wind data is used to simulate wind power generation. Wind speed is modeled via a kernel density estimator to benefit the most from the data. The obtained results indicate that the renewable energy technologies enable outcomes with significant reduction to CO_2 emissions. However, at the current prices of these technologies, operating a low emitting field links to the loss of a significant share of the expected profits.

Keywords: Offshore energy hub, energy storage, wind power, CO_2 emissions, oil production

NOMENCLATURE

Abbreviations

O&G	Oil and gas
NPD	Norwegian Petroleum Directorate
NPC	Norwegian Continental Shelf
GT	Gas turbine
OEH	Offshore energy hub
MILP	Mixed-integer linear programming
WT	Wind turbine
FPSO	Floating production storage and offloading
NPV	Net present value
RET	Renewable energy technologies
OWPP	Offshore wind power plant
STD	Standard deviation
KDE	Kernel density estimator
PDF	Probability density function
LHS	Latin Hypercube Sampling
QMC	Quasirandom Monte Carlo
CAPEX	Capital expenses
OPEX	Operational expenses
DRILLEX	Drilling expenses

Variables

λ	Average failure rate of WTs [occurrences/year]
b_{eof}	Battery end-of-life criterion
b_{lt}	Battery lifetime [years]
b_{cap_0}	Battery initial capacity [MWh]
b_{cap_d}	Battery capacity at the end of day d [MWh]
$OWPP_C$	OWPP CAPEX [$]
n_{wt}	Number of WTs
P_{wt}^{nom}	Nominal power of the WTs [MW]
$\overline{NPV}$	Mean NPV [$]
CO_2^T	Total CO_2 emissions [tonnes]
$\overline{CO_2^T}$	Mean total CO_2 emissions [tonnes]

1. INTRODUCTION

Environmental concerns surrounding our planet have been leading the world to change how to produce and consume energy. More specifically, greenhouse gas emissions have been receiving an ever-growing attention. For instance, by 2050, Europe has the ambitious goal of becoming climate neutral [1]. Several sectors of society have been employing different actions to help achieve such goal. In the energy context, substantial investment into renewable energy sources seek to reduce hydrocarbon-based power generation [2]. Regarding wind power generation, an offshore capacity of 35.3 GW had been installed around the globe by the end of 2020 [3]. Gulski et al. [4] claims that a 19% worldwide annual growth is to take place over the next ten years.

*Corresponding author: ramon.a.santos@ntnu.no
Documentation for `asmeconf.cls`: Version 1.32, September 26, 2023.

Wind intermittency can lead to long periods either with curtailment of surplus power or with reduction in oil/gas production due to the lack of electrical power supply. Storing energy from favorable wind periods for further utilization during unfavorable moments can minimize such events. Therefore, energy storage has shown to be pivotal for a net-zero future [5].

In the oil and gas (O&G) context, the Norwegian Petroleum Directorate (NPD) stated that 84.6% of the total CO_2 emissions on the Norwegian Continental Shelf (NCS) during 2018 came from gas turbines [6]. The combination of renewable sources and energy storage can play a crucial role in the decarbonization of the O&G industry. Such a combination has the potential of significantly reducing the need for polluting energy sources.

We define an offshore energy hub (OEH) as a setup that combines offshore renewable energy sources with storage components and converters. In an OEH, it is necessary to properly size the wind power plant and the storage devices. Such a task aims at obtaining the capacity values that are likely to achieve the established objectives with optimized investment decisions.

Gabrielli et al. [7] investigated the operation and design of multi-energy systems considering seasonal storage via batteries and electrolyzers. The authors proposed two approaches to select representative days and determine the technologies sizes in reasonable time. Under the assumption that the historical data represent the uncertainties, the authors treated power and heat demands, solar irradiation and energy prices deterministically. For one of the case studies, the authors highlighted that seasonal storage has the potential of greatly reducing costs and emissions compared to traditional systems.

Eladl et al. [8] optimized the configuration and operation of onshore energy hubs. The goal was to maximize social welfare while minimizing emissions. Probability density functions estimated the power generated by wind and solar sources. The study indicated that there are economic advantages in using hubs to interconnect the different sources and drains of energy.

Weimann et al. [9] analyzed the interactions among wind and solar generation, battery storage, and power to hydrogen via a mixed-integer linear programming (MILP) formulation. The authors argued that batteries and power to hydrogen are complementary if electrolizers can operate flexibly. In addition, they claimed that power to hydrogen is more beneficial when attending a H_2 demand rather than balancing the electrical grid.

Zhang et al. [10] studied OEHs in the context of a zero-emission energy supply on the NCS. An offshore energy model for investment planning and operation optimization sought decarbonization at minimum costs. A MILP formulation described the deterministic problem. The authors claim that offshore wind integration and power from shore can more than halve current emissions, depending on the taxation. However, storage may be necessary for zero-emission production.

Chapaloglou et al. [11] executed a stochastic storage sizing optimization for isolated systems. From a large number of wind generation and power demand scenarios, a non-parametric approach optimally selected a small number of scenarios that properly represented the historical data. The method outperformed other scenario selection alternatives by providing a sizing solution that is less vulnerable to the uncertainties.

This paper assesses different alternatives for the quantity of wind turbines (WTs) and for the size of batteries, electrolyzers and fuel cells. These components supply electrical power to a floating production storage and offloading (FPSO) unit. We analyze the problem from the economic and environmental perspectives. The former is quantified according to the net present value (NPV) of the synthetic project, whereas the latter corresponds to CO_2 emissions. We formulate the problem with four sets of uncertainty: oil price, FPSO electrical power demand, wind speed, and availability of WTs. We represent the reservoir characteristics deterministically, which leads to a static oil production profile. In future research, we intend to address this limitation by including uncertainties from the reservoir porosity, oil originally in place, among others. These are also relevant factors that affect the expected NPV distribution.

We model battery degradation, which is often neglected by the literature. For instance, this characteristic is not addressed in [7–11]. Our approach diverges from the reviewed papers [7–11] as they either take a deterministic route [7, 9, 10] or do not capture all the mentioned uncertainties plus the degradation characteristic [8, 11]. As a remark, Eladl et al. [8] modeled uncertainties from solar energy sources. However, this technology is not part of the system analyzed in this paper. Therefore, we propose a probabilistic assessment method that simultaneously addresses the uncertainties mentioned in the previous paragraph via quasirandom Monte Carlo simulations [12].

Section 2 of this paper describes the problem. Section 3 presents the proposed approach. Section 4 provides results and discussions. Section 5 concludes the work.

2. PROBLEM DESCRIPTION

Decarbonizing the O&G sector is part of the efforts towards a more sustainable and environmental-friendly future. OEHs have the potential to contribute to such a goal given the clean process of offshore wind power generation. In this work, we aim at assessing the economic feasibility and the environmental benefits of including WTs, Li-ion batteries, polymer electrolyte membrane electrolyzers and fuel cells to function as an OEH. These components shall power an FPSO that is planned to produce oil on the North Sea. Thus, here we address a greenfield system. Water injection into the reservoir shall help achieve the desired production rate levels. Energy storage can occur either via batteries or green hydrogen (water electrolysis fed by renewable power). The sole purpose of energy storage is to secure power for the FPSO during unfavorable wind scenarios. Gas turbines (GTs) serve as backup power sources when energy storage plus wind are not enough to cover the share of the load that must be met. Water injection is reduced if the power supply does not meet the power demand. However, if the difference between supply and demand is greater than the power required by water injection, the GTs secure adequate operation. Figure 1 depicts the studied system.

One might wonder why to consider installing fuel cells if GTs are part of the system. After all, the produced hydrogen could feed the GTs, thus dismissing the fuel cells. However, Section 3 will explain that our approach sizes the GTs according to the need of backup power over the field lifetime. Initially, we contemplate the possibility of GTs not being required depending on the sizes

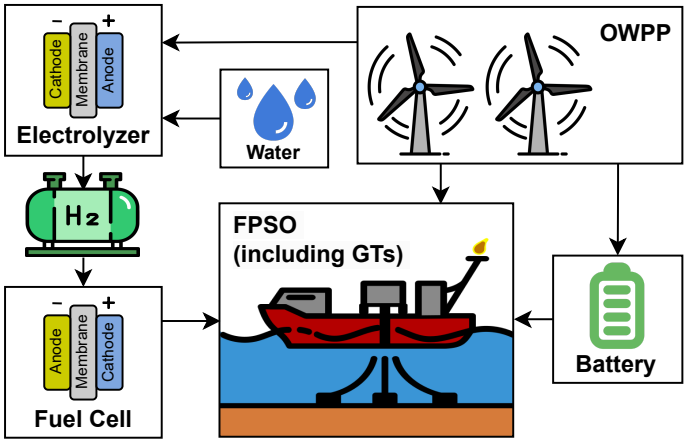

FIGURE 1: SYSTEM REPRESENTATION

of the energy storage devices and on the amount of WTs. For this reason, we consider fuel cells as potential components.

From a set of input data, we seek to analyze the trade-offs between NPV and CO_2 emissions given the sizes of the renewable energy technologies (RET) prone to installation. Figure 2 shows the inputs and main outputs of the method proposed in this paper. We discuss each of them throughout the study.

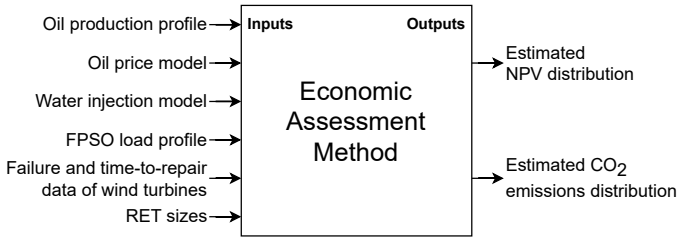

FIGURE 2: DIAGRAM OF INPUTS AND OUTPUTS

Figure 3 provides the expected instantaneous production profile of the field together with offloading information. As seen, production is expected to start 2 years after the beginning of the field construction. Furthermore, the average offloading frequency of the FPSO varies according to the production rate. Such information impacts the expected power demand since the offloading process requires a significant amount of power.

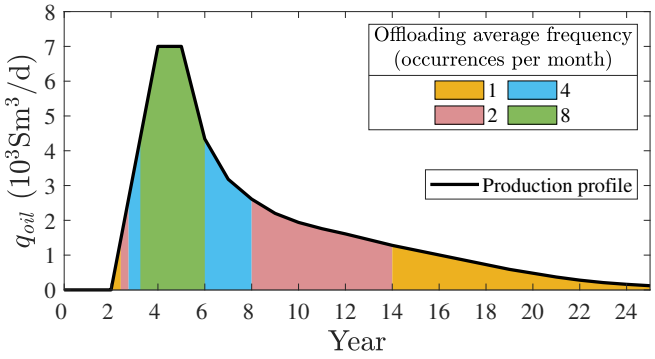

FIGURE 3: EXPECTED PRODUCTION PROFILE

We model water injection based on [13]. We consider the requirement of a water injection rate of 11000 Sm^3/d to keep the reservoir pressure at the percentage level needed to produce the expected oil rate. Lower water injection rates imply reductions in reservoir pressure. The surface in Fig. 4 illustrates this relation. In Fig. 4, the continuous lines are from [13], whereas the dotted extensions and the surface are adapted. We obtained the surface by fitting a polynomial to the lines plus extensions. This function is linear in q_w and cubic in t. Equation 1 describes the surface.

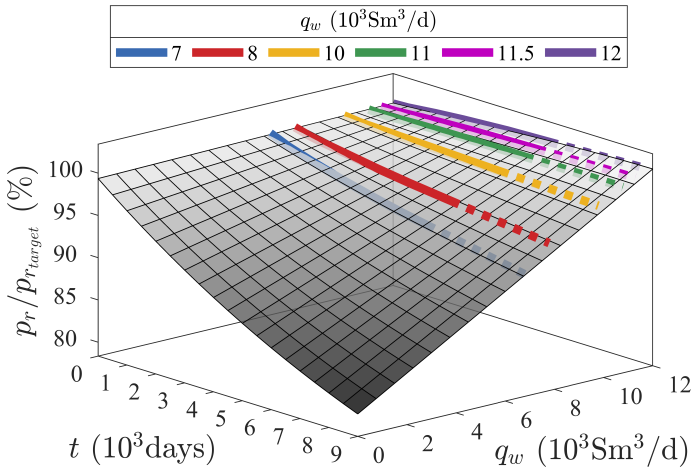

FIGURE 4: PERCENTAGE RESERVOIR PRESSURE AS A FUNCTION OF TIME AND WATER INJECTION RATE (BASED ON [13])

$$\frac{p_r}{p_{r_{target}}} = \frac{p_1 + p_3 q_w + t\left[p_2 + p_5 q_w + t\left(p_4 + p_7 q_w + p_6 t\right)\right]}{p_1 + p_3 q_w^r + t\left[p_2 + p_5 q_w^r + t\left(p_4 + p_7 q_w^r + p_6 t\right)\right]} \quad (1)$$

where: $p_1 = 3.17 \cdot 10^2$, $p_2 = -9.13 \cdot 10^{-3}$, $p_3 = 1.48 \cdot 10^{-4}$, $p_4 = 3.39 \cdot 10^{-7}$, $p_5 = 8.18 \cdot 10^{-7}$, $p_6 = -5.34 \cdot 10^{-12}$, $p_7 = -2.50 \cdot 10^{-11}$, q_w is the water injection rate (Sm^3/d), q_w^r is the target water injection rate of 11000 Sm^3/d, and t is the time (days).

Figure 4 reveals that the impact of water injection also depends on how much time has passed since the beginning of production. To translate the percentage reservoir pressure reduction to the oil rate, we assume an affine relation. For instance, a reduction of 10% in pressure grants a 10% smaller oil rate compared to the expected production profile.

A limitation of our water injection model relates to a loss of reservoir resources. The following happens in our model when we reduce water injection. Some of the anticipated oil is not extracted since the oil rate is lower than the one in the production profile. This share is taken as lost due the fact that we base our production rates on time instead of oil in place. In reality, the extraction of this portion would be postponed. Despite this limitation, our model is on the conservative side since we are underestimating NPV. If the delayed production had been considered, the delayed volumes of oil in the production profile would have moved towards the tail of the profile. At the tail, the resulting income would be heavily discounted, and the resulting effect on the NPV could be approximated as lost production.

The field is expected to demand 15 MW as base electrical power for the daily operations. However, this value grows linearly over time due to the intensification of separation processes,

which relates to the ever-increasing water-cut. By the end of the field maximum lifetime, the load is antecipated to be at 19.5 MW. Furthermore, over the whole period of operations, the load can vary by up to 20% above the base value given the variability of several factors, such as maintenance activities and unexpected power demand from compressors. Lastly, offloading events require 2 additional MW over the day in which they occur. Figure 5 visually represents the aforementioned information, except for the offloading power demand.

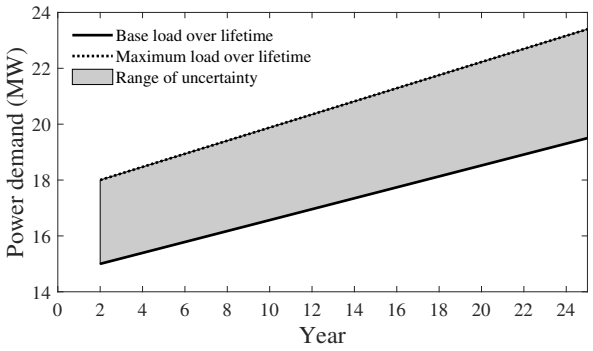

FIGURE 5: EXPECTED LOAD OVER THE FIELD LIFETIME

To model wind profiles, we collected open data from [14], and utilized wind speed historical measurements at 100 meters height for the Anholt offshore wind power plant (OWPP). The samples date from 01.01.2013 to 31.12.2014. Ørsted provides mean speed values together with the standard deviation (STD) in a resolution of 10 minutes. Thus, we modeled a kernel density estimator (KDE) to capture the uncertainty of the data. The STD values were used to determine the bandwidths for the KDE. Figure 6 reveals that our estimator more accurately represents the dataset compared to the Weibull probability density function (PDF). As a support to our approach, Han et al. [15] claim that KDE tends to outperform parametric functions when fitting wind power distributions and estimating wind power density.

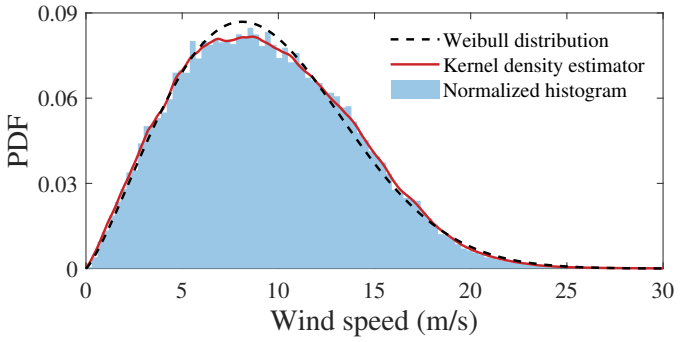

FIGURE 6: WIND SPEED MODEL

From the inputs presented, we seek to assess the economic viability of WTs, batteries, electrolyzers, fuel cells, and hydrogen storage as an OEH to power the FPSO. Such an assessment highly depends on the size of the components since they impact the capital expenditures and the energy availability over the field lifetime. In the following section, we present our approach.

3. PROPOSED APPROACH

Given that the renewable technologies can be sized within established ranges, we apply a statistical approach to carry out the economic and environmental assessment according to different sizing possibilities. The quantity of WTs can vary from 2 to 10. The storage capacity of the batteries can range from 0 to 200 MWh. The power of the batteries, electrolyzers and fuel cells can vary from 0 to 20 MW. Although 200 MWh is a high value, the constant development of batteries indicate that such a magnitude can become realizable soon. Even today, there is a battery storage case featuring 180 MWh of storage capacity [16]. We consider that the batteries, electrolyzers and fuel cells have lifetimes of 12 years. Therefore, we consider two sets of each of these technologies so that we cover the whole production horizon, which we assume not to be longer than 23 years.

We utilize the low discrepancy quasirandom sampling from https://github.com/SciML/QuasiMonteCarlo.jl to obtain sizing combinations that adequately span the possible region. Quasirandom sampling outperforms pseudorandom in many applications [12]. Thus, this approach is more likely to cover a wide range of RET combinations. Figure 7 exemplifies different sampling techniques, including Latin Hypercube Sampling (LHS). The figure demonstrates how a quasirandom approach can more effectively spread the same quantity of samples over the region.

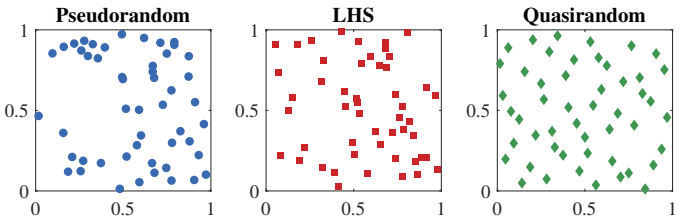

FIGURE 7: EXAMPLE OF DISTINCT SAMPLING METHODS

From the previous explanation, we created 10000 RET samples given the presented sizing ranges. We highlight that the samples originally belong to $\mathbb{R}$. Hence, we round the numbers to obtain integer capacity and power values, in addition to the number of WTs (n_{wt}). We then subject each sample to a quasirandom Monte Carlo simulation (QMC) with daily resolution. The QMC returns the expected NPV and total CO_2 emissions of the system.

On top of the power demand and wind power uncertainties, our approach accounts for two other sources of uncertainty. The oil price is an important factor that greatly impacts NPV. We model its uncertainty by considering different price trajectories over the years. WTs availability is an uncertainty usually neglected in the literature that addresses OEHs studies, as in [7–11]. Our QMC approach enables the modeling of WTs failures and availability given average failure rates and time to repair. Figure 8 exhibits a flowchart of the QMC method. As a sequence, we explain the steps of the process. As an observation, our study neglects any transient behavior. Since we consider a daily resolution, we assume 24 hours to be considerably longer than the dynamics of any equipment of the system.

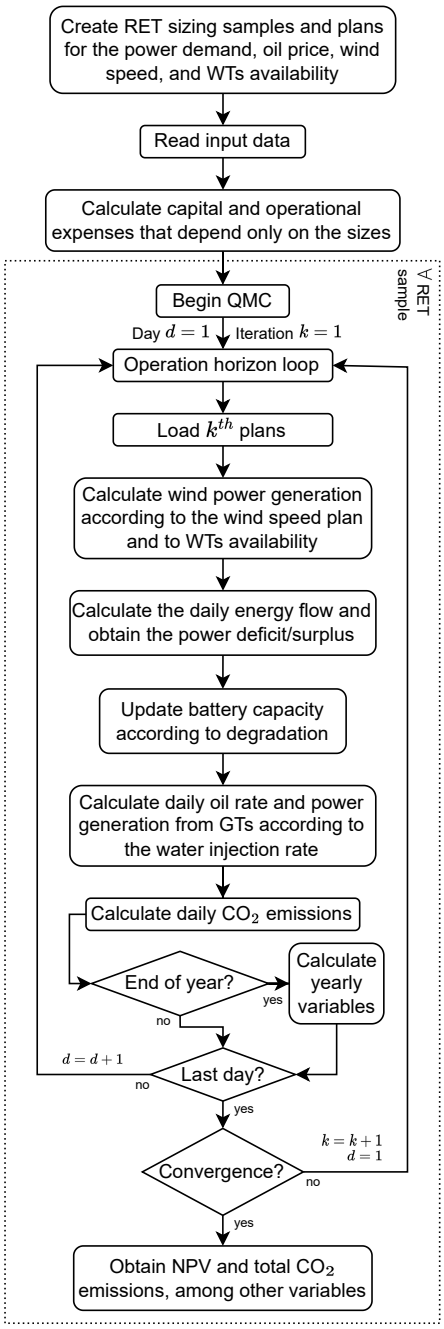

FIGURE 8: HIGH LEVEL FLOWCHART OF THE METHOD

- Initially, we obtain the RET sizing samples according to the quasirandom approach previously described, thus obtaining a large set of possible combinations. We highlight that a particular combination not necessarily corresponds to a realistic sizing alternative. Still, further ahead we show that spanning the solution region allows our method to "look" at all combinations and estimate their economic feasibility and level of emissions. Consequently, unrealistic combinations tend to grant poor trade-offs between NPV and CO_2 emissions. The opposite is true for combinations that are more meaningful in reality. Or for combinations in which a certain unrealistic characteristic only slightly affects NPV, e.g., an over-sized electrolyzer.

- Given that we execute a QMC for each RET sample, we create plans/samples for the four addressed sets of uncertainty. In other words, the power demand, the wind speed, the oil price, and the availability of the WTs. Each plan for each uncertainty set covers the 8395 days (23 years) of operation. We created 300 different quasirandom plans to be the inputs to the QMC iterations of all RET samples. However, the number of required plans depends on the attendance of the convergence criterion. Below we explain how we address each uncertainty set.

  – Power demand: for each day of the operation horizon, we draw a sample from a uniform distribution that ranges from the base load to the maximum contingency shown in Fig. 5.

  – Wind speed: from the kernel density estimator of Fig. 6, we randomly pick an original data point. Then, we draw a sample from the normal distribution defined by the mean and STD values provided in the dataset. This is the standard approach to draw samples from a KDE.

  – Oil price: we apply a mean reversion predictor to generate several oil price trajectories over the operation horizon. This generator is openly available at [17].

  – WTs availability: at each day, we randomize a number in [0,1] for each WT in the RET sample. If Eq. 2 is true, the WT is set as unavailable for 3 days, which is the mean time to repair considered in this paper.

$$rand \leq \lambda/365, \tag{2}$$

  where: λ is the average failure rate, taken as equal to 6 occurrences per year [18].

- We read the RET samples, the plans for the uncertainty sets, and the RET economic and technical data necessary to quantify NPV. Table 1 provides such data together with the base sources. It is noteworthy that we assume the installation costs of the RET components to be part of the respective CAPEX. Further below we mention considerations about some of the data.

  – Battery end-of-life criterion (b_{eof}): according to [20], a simplistic modeling of batteries leads to significant overestimation of battery-related revenues. The authors claim that neglecting capacity degradation is the main aspect regarding this issue. Therefore, we model calendar degradation as in [20]. Equation 3 describes such phenomenon and shows that the battery capacity is expected to degrade 2% per year throughout its lifetime (b_{lt}) of 12 years.

$$b_{cap_d} = b_{cap_0} \cdot \left[1 - \left(1 - b_{eof}\right) \cdot \frac{d}{365 b_{lt}}\right], \tag{3}$$

  where: b_{cap_d} is the battery capacity at the end of day d, and b_{cap_0} is the initial capacity that comes from the RET sample.

  – Battery CAPEX: this parameter varies significantly in the literature. References [19, 20, 26] provide average values of 600 to 800, 165 and 137 $/kWh, respectively. Furthermore, reference [26] claims that the average price will be approximately 100 $/kWh in 2023. From the industrial experience of the fourth author of this paper, here we consider the value shown in Table 1.

TABLE 1: ECONOMIC AND TECHNICAL DATA

Datum	Value
Battery storage and recovery efficiency	0.9 [19]
Battery end-of-life criterion	0.76 [20]
Battery CAPEX	250 $/kWh
Battery fixed OPEX	8 $/kWyear [20]
Battery variable OPEX	2.3 $/discharged MWh [20]
Electrolyzer efficiency	0.65 [21]
Fuel cell efficiency	0.55 [21]
Electrolyzer CAPEX	0.7 M$/MW [22]
Electrolyzer OPEX	2% of CAPEX/year [22]
Electrolyzer stack lifetime	50000 hours [22]
Electrolyzer stack CAPEX	0.21 M$/MW [22]
Fuel cell CAPEX	2 M$/MW [22]
Fuel cell OPEX	4% of CAPEX/year [22]
Fuel cell stack lifetime	15000 hours [22]
Fuel cell stack CAPEX	50% of CAPEX [22]
H_2 stationary storage CAPEX	470 $/kg$H_2$ [22]
H_2 stationary storage OPEX	2% of CAPEX/year [22]
H_2 stationary storage maximum capacity	10000 kg [21]
H_2 conversion for liquid storage	10.3 kWh/kg [21]
Gas turbine CAPEX	1000 $/kW [23]
Gas turbine OPEX	10 $/produced MWh
Wind turbine unit CAPEX	1.3 M$/MW [24]
Wind turbine OPEX	15 $/produced MWh [24]
Wind power plant CAPEX	$4.9 \cdot n_{wt} \cdot P_{wt}^{nom}$ M$ [25]

  - Wind power plant CAPEX ($OWPP_C$): in [25], percentage costs of a variety of OWPP components and processes are found. For instance, the purchase and installation of cables, overall maintenance, and WTs towers, to name a few. To quantify $OWPP_C$, we considered that the WT CAPEX from [24] corresponds to the nacelle, rotor, and tower of [25]. By consulting these references, one concludes that we are taking the CAPEX of WTs (Eq. 4) as 19.2% of $OWPP_C$. We subtracted the operation and maintenance percentages (28.2% of $OWPP_C$ [25]) since we are accounting for capital expenditures. Therefore, we approximated $OWPP_C$ according to Eq. 5. We assumed the remaining value (Table 1) as the $OWPP_C$ cost per MW, i.e., the purchase plus installation cost of the substation, cables, converters, and WTs.

$$\text{CAPEX of WTs} = 1.3 \cdot 10^6 \cdot n_{wt} \cdot P_{wt}^{nom}, \tag{4}$$

    where: P_{wt}^{nom} is the nominal power of the WTs.

$$OWPP_C = \frac{\text{CAPEX of WTs}}{0.192} \cdot (1 - 0.282) \tag{5}$$

- Apart from the expenses-related information so far disclosed, the expected O&G CAPEX plus DRILLEX is equal to 250 M$ in year 1 and 500 M$ in years 2 and 3. These expenditures relate to the purchase and installation of the O&G components, in addition to the drilling activities. The costs were quantified based on estimations of the overall equipment weight. We do not detail weight and cost estimation regarding the FPSO components as this task escapes the scope of this paper. Table 2 provides the O&G production OPEX. The expected decommissioning and abandonment (D&A) cost is equal to 50 M$. D&A occurs in the year that follows the last year of production.

TABLE 2: OPEX (M$) FROM O&G

Y	OPEX	Y	OPEX	Y	OPEX	Y	OPEX
3	30	9	26.3	15	23.3	21	21.1
4	40	10	25.5	16	22.9	22	20.8
5	40	11	25	17	22.5	23	20.6
6	32.4	12	24.6	18	22.1	24	20.5
7	29.1	13	24.1	19	21.7	25	20.3
8	27.5	14	23.7	20	21.4	-	-

- We model CO_2 taxation similarly to [27]. Current CO_2 taxation in Norway is at approximately 70.5 $/tonne$CO_2$ [28], assuming, for simplicity, a NOK to USD conversion of 10 to 1. According to [27], the Norwegian CO_2 taxation will increase to 200 $/tonne$CO_2$ by 2030. Hence, we linearly increase the yearly taxation from 70.5 $/tonne$CO_2$ in 2022 (taken as year 1) to 200 $/tonne$CO_2$ in 2030. Then, as in [27], we keep it constant for the remaining operation horizon.

- As seen in Table 1, most of the costs can be calculated based on the size of the components. Thus, we quantify part of the investment according to the RET sample. Such procedure is not valid for the batteries variable OPEX, the total costs with electrolyzers and fuel cells stacks, and the WTs OPEX. These variables depend, respectively, on the discharged energy, number of replacements according to lifetime, and produced energy. In other words, they relate to the operation of the components. Hence, we calculate them over each QMC iteration.

- For every RET sample, we run a QMC to estimate the NPV and the total CO_2 emissions $\left(CO_2^T\right)$. For each iteration of this process, we load a different plan for the power demand, wind speed, oil price, and WTs availability. Therefore, we sweep different possibilities for the realizations of the uncertainties. These plans cover the whole period of production. Hence, each iteration provides one NPV and CO_2^T estimation for a RET sample. As convergence criterion for each QMC simulation, we perform the following procedure: (i) for every iteration n, except for the first, we calculate the mean NPV and CO_2^T based on the NPV and CO_2^T estimations from iterations 1 to n, which we refer to as m_1; (ii) we compare this calculation to the mean NPV and CO_2^T based on the estimations from iterations 1 to n-1, which we refer to as m_2; (iii) if for both NPV and CO_2^T Eq. 6 is true, we assume that the simulations have converged. We consider that variations within 0.1% relative to the previous iteration are negligible. Thus, additional iterations would have minor impact on the mean (expected) NPV and CO_2^T.

$$\frac{|m_1 - m_2|}{m_1} < 0.001 \tag{6}$$

- At each day, we calculate the generated wind power based on the daily wind speed and availability of the WTs. For this task, we consider the power curve of the Siemens Gamesa 8 MW model presented in [29]. In addition, we account for wake effects to avoid overestimating the wind energy generation. We multiply all wind power calculations by 0.9, thus considering a 10% loss due to wake effects. This is a conservative estimation since such losses are slightly larger than the ones reported in some studies [30, 31], assuming optimized layouts for the WTs.
- The energy flow calculation depends on the wind generation:
  - If the available wind power is greater than the load, the power surplus charges the battery. If the surplus exceeds the battery power rating and/or if it is more than enough to reach maximum battery capacity, the remaining power produces hydrogen. This priority order follows the efficiency of the energy conversion processes.
  - In opposition, if the available wind power is less than the load, the battery supplies power to the FPSO. If the power deficit exceeds the battery power times the recovery efficiency and/or if the it is enough to empty the battery, hydrogen provides power according to the stored H_2 and to the fuel cell power rating and efficiency.
- In the second situation of the previous item, the energy sources may not be able to fully attend the load. In such a case, water injection can be reduced to decrease the power demand. From Fig. 4, the target water injection rate of 11000 Sm^3/d relates to a power of 3.8 MW. We assume a linear relation to determine the water injection reduction. For instance, if the load surpasses the supply by 1.9 MW, the water injection rate is reduced to 5500 Sm^3/d. If the demand exceeds the supply by more than 3.8 MW, water injection is interrupted, and the GTs provide the power that transcends this value. Therefore, over the 23 years of production, we verify which was the greatest power required from the GTs to estimate the power rating to be purchased.
- For each day, we adjust the oil rate from the production profile (Fig. 3) according to the water injection rate through Eq. 1. As a reminder, we assume a linear relation between the reservoir pressure reduction and the production rate reduction. In addition, we calculate the battery degradation using Eq. 3. Lastly, we estimate the daily CO_2 emissions. Based on the input from the fourth author of this paper, we take CO_2 emissions from GTs as 650 kg/MWh. Given that NPD claimed CO_2 emissions from GTs to be 84.6% of the total emissions [6], the remaining sources of CO_2 correspond to 15.4% of the total. Therefore, we take the total emissions as equal to the GTs emissions divided by 0.846. Then, we multiply the total by 0.154 to estimate emissions from other sources.
- Over the 8395 days of a QMC iteration, we calculate the yearly variables by the end of each year: (i) in our model, the battery has an OPEX share that depends on the discharged energy. We calculate this portion at each year to adequately calculate its influence on NPV; (ii) at each day, we perform cumulative sums to store operation hours of the electrolyzers and fuel cells stacks. Upon replacement of a stack, we add the cost to the associated year; (iii) analogously to the battery variable OPEX, the WTs OPEX depends on the produced energy. Thus, we account for such costs by the end of each year; (iv) by the end of each production year, all daily oil rates are summed up. The resulting annual oil volume is sold in the following year. The impact on NPV depends on the oil prices in place.
- After sweeping all 8395 days, we verify if the process has converged (Eq. 6). If negative, we proceed to the next iteration with new plans for the uncertainty sets. If positive, the simulation for the current RET sample is over. The interest rate for the NPV calculations is equal to 7%. The production profile estimates 23 years of maximum production. However, by the end of each year, we verify if the discounted revenue is positive. If it is not, we adjust the last year of operation so that production occurs for as long as there are positive discounted revenues.

The described procedure provides distributions of NPV and CO_2^T for each RET sample, according to the calculations from each iteration. For every sample, we estimate the expected values for the mentioned variables by taking the mean of all computed NPV $\left(\overline{NPV}\right)$ and CO_2^T $\left(\overline{CO}_2^T\right)$ within the distributions. The next section presents the results for the system under study.

4. RESULTS AND DISCUSSIONS

We applied the method from the previous section to the FPSO plus OEH described in Section 2. Apart from the 10000 RET samples, we simulated configurations that have WTs, but no storage. In addition, we evaluated situations where the power supply comes fully from GTs. Such simulations assume that the GTs provide the power required by the water injection process. For the scenario fully dependent on GTs, we considered two simulations. One applies the growing CO_2 taxation described in the previous section. The other takes a constant 70.5 \$/tonne CO_2 taxation. Across all samples, the mean, STD, minimum and maximum number of iterations required for convergence are equal to 70.33, 24.02, 37 and 137, respectively.

Figure 9 presents the trade-off between $\overline{NPV}$ and $\overline{CO}_2^T$ for all samples under analysis. As observed, Fig. 9 presents a sensitivity analysis on the CAPEX of all renewable energy components. Figure 9(b) considers a 25% higher CAPEX compared to the prices from Table 1. The regular prices relate to Fig. 9(c). In Fig. 9(d), RET CAPEX is 25% lower. As a sequence, we enunciate a series of discussions related to Fig. 9.

The solution that relies only on GTs as energy supply and follows a constant CO_2 taxation is the most profitable. The $\overline{NPV}$ of this solution is equal to $1.5373 \cdot 10^9$\$. Furthermore, this solution is the most polluting in terms of CO_2, as expected. Its $\overline{CO}_2^T$ is equal to $2.3668 \cdot 10^6$ tonnes. When the growing CO_2 taxation is introduced, overall emissions reduce since the taxes tend to cause negative revenues to occur earlier. Hence, the field profitable period tends to shorten.

The GTs-based solution with growing CO_2 taxation indicates that tax policies can play a relevant role in the decarbonization of the offshore O&G sector. For the cases with regular and decreased RET CAPEX, some of the RET samples have higher $\overline{NPV}$ than the GTs-based sample, despite indicating lower $\overline{CO}_2^T$. For instance,

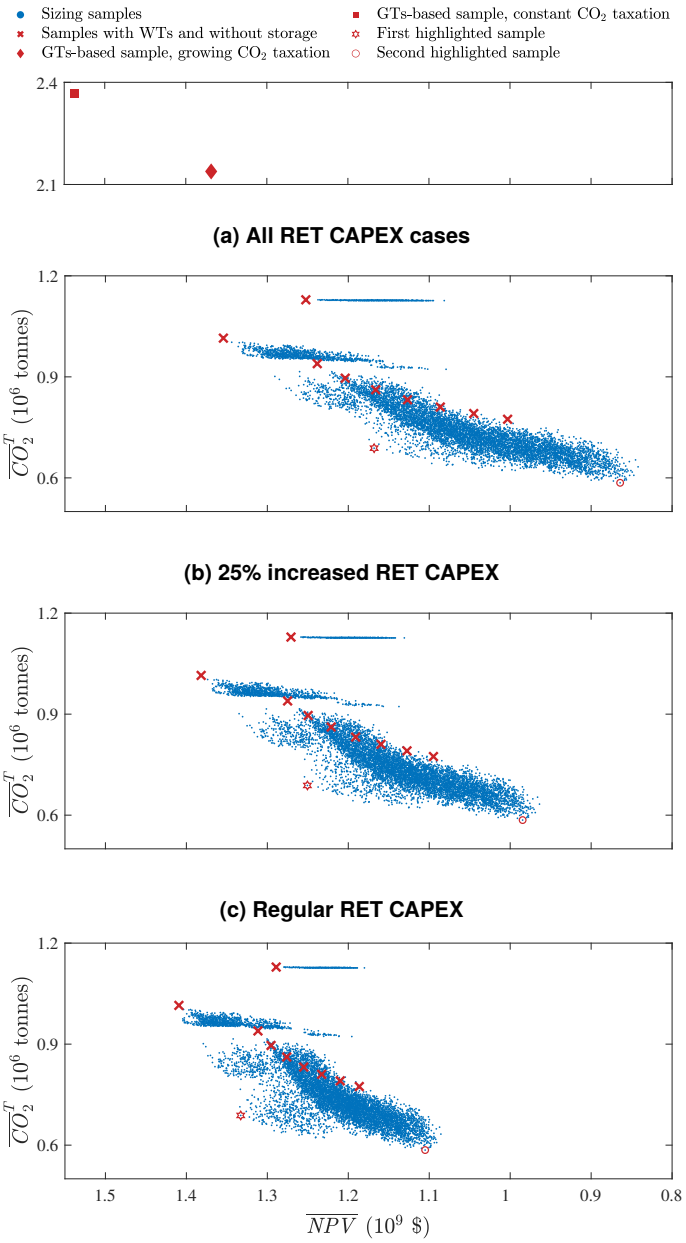

(a) All RET CAPEX cases

(b) 25% increased RET CAPEX

(c) Regular RET CAPEX

(d) 25% decreased RET CAPEX

FIGURE 9: ENVIRONMENTAL AND ECONOMIC TRADE-OFFS

take the sample with 3 WTs and no energy storage (west most "x") in the case with regular RET CAPEX. This sample provides a 1% higher $\overline{NPV}$ and a 53% lower $\overline{CO_2}^T$ compared to the GTs-based sample. Thus, our results indicate that the future taxation on CO_2 can enable RET-based solutions that would be economically disadvantageous in the current taxation scenario.

The sample with 3 WTs and no energy storage has the highest $\overline{NPV}$ among the RET samples. However, most of the other RET samples dominate it in terms of $\overline{CO_2}^T$. Such a result indicates that energy storage is key to a net-zero future. In fact, several studies on this topic have come to this conclusion, such as [5, 10, 32, 33].

The analyses ahead regard the case with regular RET CAPEX. Figure 9 highlights two among the non-dominated RET samples. The first and second present 10% and 29% lower $\overline{NPV}$ compared to the most profitable sample, respectively. They show 68% and 73% lower $\overline{CO_2}^T$, respectively, compared to the GTs-based sample with growing CO_2 taxation. Although the second highlighted sample is the least CO_2 emitting one, changing from the first to the second heavily impacts $\overline{NPV}$. In connection with this statement, Fig. 9 enables the estimation of the CO_2 mitigation costs. Let us compare the GTs-based sample with growing CO_2 taxation to the first highlighted sample. On the one hand, the 118 M\$ reduction in $\overline{NPV}$ from the former to the latter leads to a decrease of $1.4501 \cdot 10^6$ tonnes in $\overline{CO_2}^T$. Thus, the mitigation cost is equal to 81 \$/tonneCO_2. On the other hand, this cost raises to 2586 \$/tonneCO_2 when the first highlighted sample is compared to the second. Therefore, one can notice that moving from the more to the less CO2-emitting combinations causes the mitigation cost to increase significantly. We provide additional information about the first highlighted sample in Appendix A.

The second highlighted sample estimates CO_2 emissions to reach $5.8540 \cdot 10^5$ tonnes over the field lifetime. As described in Section 2, our model considers a share of emissions that do not relate to the GTs. This portion represents pollution that cannot be totally avoided unless carbon capture and storage technologies are installed. These emissions are equal to $4.5696 \cdot 10^5$ tonnes. Looking at the emissions of the second highlighted sample, one concludes that no sample was capable of dismissing the GTs. Such a result indicates that larger storage capacities might be needed to enable zero emissions from GTs.

As stated in Section 3, we size the GTs based on their maximum power generation over a QMC iteration. The GTs-based sample with constant CO_2 taxation is the one which exploits GTs the most. Its mean GT CAPEX is equal to 24 M\$. Among all RET samples, the lowest mean GT CAPEX is equal to 19 M\$. Such a fact leads to the conclusion we believe is the most important in this study. It indicates that even a low emitting system may need significant power capacity from GTs due to the intermittency of wind. To secure power supply and guarantee the continuity of critical processes in oil production, our results suggest that GTs are needed during unfavorable wind scenarios in which energy storage has been depleted. However, this item requires further investigation. Additional storage capacity could lead to scenarios where GTs are not required, although other challenges would probably arise. For instance, weight limitation might make it unfeasible to install certain storage capacities offshore.

In general, our results indicate that the growing CO_2 taxation tends to enable solutions that greatly reduce CO_2 emissions compared to a setup based only on power from GTs. Furthermore, the trend of reduced RET costs contribute to making OEHs economically viable. Still, for our system, significantly reducing CO_2 emissions requires the sacrifice of a share of the profits.

In future research, we intend to: (i) model water injection as dependent on the oil in place instead of time. By doing do, we can represent the fact that oil unexploited due to lack of water injection has its production delayed rather than lost; (ii) investigate how the varying water injection affects the dynamics of the reservoir, and seek to understand if our method would benefit from

modeling this behavior; (iii) add uncertainties of the oil reservoir to our method, e.g., the oil originally in place. Such inclusions are likely to improve how we capture the uncertainties from NPV and CO_2 emissions; (iv) analyze the details behind the estimation of weight, required area, and purchase plus installation costs of the oil producer components, e.g., the marine structure. Such an analysis could help us detect additional uncertainties that deserve attention; (v) extend the previous item to the RET components, specially the batteries, thus helping us evaluate the storage capacity limitation according to the feasible size and weight of the battery pack. In addition, this task would enable us to verify the more volatile prices that are worth subjecting to sensitivity analyses; (vi) investigate potential operation and maintenance requirements due to the marine environment; (vii) add the possibility of exporting hydrogen through pipelines to attend onshore demands, and quantify the profitability of this process; (viii) analyze other energy storage alternatives such as compressed air and liquid metal batteries; (ix) thoroughly investigate the dynamics of the RET equipment, thus seeking to determine at which resolution they should be considered; (x) apply our method to a brownfield system, and assess if installing an OEH and/or importing power from shore would be beneficial; (xi) study if and how our assessment method can evolve to a sizing tool. In other words, we want to search how to polish the most promising samples through local optimization. This approach would search the vicinity of a sample and find an optimal sizing solution regarding the RET components.

5. CONCLUSION

This paper presented a probabilistic assessment concerning the economic viability of an offshore energy hub to supply electrical power to an oil producing FPSO on the North Sea. The proposed method enabled us to capture a variety of uncertainties that affect the NPV and CO_2 emissions estimations. Our results indicate that gas turbines may be necessary in a net-zero future due to the wind speed volatile behavior. Furthermore, our findings suggest that the current prices of the analyzed renewable energy technologies enable significant reduction to CO_2 emissions. The reductions to NPV occur at a less intense pace, despite not being negligible.

ACKNOWLEDGMENTS

This work was funded by the European Union's Horizon 2020 research and innovation programme under the Marie Skłodowska-Curie grant No. 956433 (H2020-MSCA-ITN-2020, Innovative Tools for Cyber-Physical Energy Systems - InnoCyPES).

REFERENCES

[1] Commission, European. "2030 Climate Target Plan." European Commission (2020). Accessed September 5, 2022, URL https://ec.europa.eu/clima/eu-action/european-green-deal/2030-climate-target-plan.

[2] Bloomberg. "Renewable Investment." Bloomberg (2022). Accessed August 20, 2022, URL https://www.bloomberg.com/graphics/climate-change-data-green/investment.html.

[3] Bilgili, Mehmet and Alphan, Hakan. "Global growth in offshore wind turbine technology." *Clean Technologies and Environmental Policy* (2022): pp. 1–13DOI 10.1007/s10098-022-02314-0.

[4] Gulski, E, Anders, GJ, Jongen, RA, Parciak, J, Siemiński, J, Piesowicz, E, Paszkiewicz, S and Irska, I. "Discussion of electrical and thermal aspects of offshore wind farms' power cables reliability." *Renewable and Sustainable Energy Reviews* Vol. 151 (2021). DOI 10.1016/j.rser.2021.111580.

[5] Machlev, R, Zargari, N, Chowdhury, NR, Belikov, J and Levron, Y. "A review of optimal control methods for energy storage systems-energy trading, energy balancing and electric vehicles." *Journal of Energy Storage* Vol. 32 (2020). DOI 10.1016/j.est.2020.101787.

[6] NPD. "Emissions, discharges and the environment." Norwegian Petroleum Directorate (2020). Accessed August 16, 2022, URL https://www.npd.no/en/facts/publications/reports/resource-report/resource-report-2019/emissions-discharges-and-the-environment/.

[7] Gabrielli, Paolo, Gazzani, Matteo, Martelli, Emanuele and Mazzotti, Marco. "Optimal design of multi-energy systems with seasonal storage." *Applied Energy* Vol. 219 (2018): pp. 408–424. DOI 10.1016/j.apenergy.2017.07.142.

[8] Eladl, Abdelfattah A, El-Afifi, Magda I, Saeed, Mohammed A and El-Saadawi, Magdi M. "Optimal operation of energy hubs integrated with renewable energy sources and storage devices considering CO2 emissions." *International Journal of Electrical Power & Energy Systems* Vol. 117 (2020). DOI 10.1016/j.ijepes.2019.105719.

[9] Weimann, Lukas, Gabrielli, Paolo, Boldrini, Annika, Kramer, Gert Jan and Gazzani, Matteo. "Optimal hydrogen production in a wind-dominated zero-emission energy system." *Advances in Applied Energy* Vol. 3 (2021). DOI 10.1016/j.adapen.2021.100032.

[10] Zhang, Hongyu, Tomasgard, Asgeir, Knudsen, Brage Rugstad, Svendsen, Harald G, Bakker, Steffen J and Grossmann, Ignacio E. "Modelling and analysis of offshore energy hubs." *Energy* Vol. 261 (2022): p. 125219. DOI 10.1016/j.energy.2022.125219.

[11] Chapaloglou, Spyridon, Varagnolo, Damiano, Marra, Francesco and Tedeschi, Elisabetta. "Data-informed scenario generation for statistically stable energy storage sizing in isolated power systems." *Journal of Energy Storage* Vol. 51 (2022). DOI 10.1016/j.est.2022.104311.

[12] Kucherenko, Sergei, Albrecht, Daniel and Saltelli, Andrea. "Exploring multi-dimensional spaces: A comparison of Latin hypercube and quasi Monte Carlo sampling techniques." *ArXiv e-prints* (2015). URL https://arxiv.org/abs/1505.02350.

[13] Kristian Engen Eide, Orkhan Ismayilov Julian Nadarzy Vegard Aleksander Amundsen Kjøsnes, Jeffrey Catterall. "Improved Oil Recovery with Water Injection." (2011). URL http://bit.ly/3CiwNsZ.

[14] Ørsted. "Wind data." Ørsted (2019). Accessed July 1, 2022, URL https://orsted.com/en/our-business/offshore-wind/wind-data.

[15] Han, Qinkai, Ma, Sai, Wang, Tianyang and Chu, Fulei. "Kernel density estimation model for wind speed probability distribution with applicability to wind energy assessment in China." *Renewable and Sustainable Energy Reviews* Vol. 115 (2019). DOI 10.1016/j.rser.2019.109387.

[16] Durakovic, Adnan. "Offshore Wind and Battery Storage Project Takes Off in Japan." Offshore WIND (2022). Accessed December 21, 2022, URL https://www.offshorewind.biz/2022/09/09/offshore-wind-and-battery-storage-project-takes-off-in-japan/.

[17] M, Stanko. "Early Field Planner." Norwegian University of Science and Technology (2021). Accessed November 23, 2022, URL http://www.ipt.ntnu.no/~stanko/files/Tools/EarlyFieldPlanner/SingleOilReservoir/v1.0/.

[18] Paul, Santanu and Rather, Zakir Hussain. "A novel approach for optimal cabling and determination of suitable topology of MTDC connected offshore wind farm cluster." *Electric Power Systems Research* Vol. 208 (2022). DOI 10.1016/j.epsr.2022.107877.

[19] Simpson, JG, Hanrahan, G, Loth, E, Koenig, GM and Sadoway, DR. "Liquid metal battery storage in an offshore wind turbine: Concept and economic analysis." *Renewable and Sustainable Energy Reviews* Vol. 149 (2021): p. 111387. DOI 10.1016/j.rser.2021.111387.

[20] Jafari, Mehdi, Botterud, Audun and Sakti, Apurba. "Estimating revenues from offshore wind-storage systems: The importance of advanced battery models." *Applied Energy* Vol. 276 (2020). DOI 10.1016/j.apenergy.2020.115417.

[21] Thommessen, Christian, Otto, Maximilian, Nigbur, Florian, Roes, Jürgen and Heinzel, Angelika. "Techno-economic system analysis of an offshore energy hub with an outlook on electrofuel applications." *Smart Energy* Vol. 3 (2021). DOI 10.1016/j.segy.2021.100027.

[22] Scolaro, Michele and Kittner, Noah. "Optimizing hybrid offshore wind farms for cost-competitive hydrogen production in Germany." *International Journal of Hydrogen Energy* Vol. 47 No. 10 (2022): pp. 6478–6493. DOI 10.1016/j.ijhydene.2021.12.062.

[23] Statista. "Forecast capital expenditure of a conventional natural gas combustion turbine power plant in the United States from 2022 to 2050." Statista (2022). Accessed December 5, 2022, URL https://www.statista.com/statistics/243704/capital-costs-of-a-typical-us-gas-turbine-power-plant/.

[24] Guard, Weather. "Wind Turbine Cost: Worth The Million-Dollar Price In 2022?" Statista (2021). Accessed November 10, 2022, URL https://weatherguardwind.com/how-much-does-wind-turbine-cost-worth-it/.

[25] Catapult. "Wind farm costs." Catapult: Offshore Renewable Energy (2022). Accessed November 10, 2022, URL https://guidetoanoffshorewindfarm.com/wind-farm-costs.

[26] Bloomberg. "Battery pack prices cited below $100/kwh for the first time in 2020, while market average sits at $137/kwh." Bloomberg (2020). Accessed December 5, 2022, URL https://about.bnef.com/blog/battery-pack-prices-cited-below-100-kwh-for-the-first-time-in-2020-while-market-average-sits-at-137-kwh/.

[27] Eyni, Leila, Stanko, Milan and Schümann, Heiner. "Methods for early-phase planning of offshore fields considering environmental performance." *Energy* Vol. 256 (2022): p. 124495. DOI 10.1016/j.energy.2022.124495.

[28] Petroleum, Norwegian. "Emissions to air." Norwegian Petroleum (2022). Accessed November 23, 2022, URL https://www.norskpetroleum.no/en/environment-and-technology/emissions-to-air/.

[29] Golroodbari, SZM, Vaartjes, DF, Meit, JBL, Van Hoeken, AP, Eberveld, M, Jonker, H and van Sark, WGJHM. "Pooling the cable: A techno-economic feasibility study of integrating offshore floating photovoltaic solar technology within an offshore wind park." *Solar Energy* Vol. 219 (2021): pp. 65–74. DOI 10.1016/j.solener.2020.12.062.

[30] Paul, Santanu and Rather, Zakir Hussain. "A new approach for selection of a suitable wind turbine for a wind farm." *2016 IEEE International Conference on Power Electronics, Drives and Energy Systems (PEDES)*: pp. 1–6. 2016. IEEE. DOI 10.1109/PEDES.2016.7914351.

[31] Wu, Yuan-Kang, Su, Po-En, Su, Yu-Sheng, Wu, Ting-Yi and Tan, Wen-Shan. "Economics-and reliability-based design for an offshore wind farm." *IEEE Transactions on Industry Applications* Vol. 53 No. 6 (2017): pp. 5139–5149. DOI 10.1109/TIA.2017.2737399.

[32] Sharma, Vanika, Haque, Mohammed H and Aziz, Syed Mahfuzul. "Energy cost minimization for net zero energy homes through optimal sizing of battery storage system." *Renewable Energy* Vol. 141 (2019): pp. 278–286. DOI 10.1109/j.renene.2019.03.144.

[33] Pimm, Andrew J, Palczewski, Jan, Barbour, Edward R and Cockerill, Tim T. "Using electricity storage to reduce greenhouse gas emissions." *Applied Energy* Vol. 282 (2021). DOI 10.1109/j.apenergy.2020.116199.

APPENDIX A. FIRST HIGHLIGHTED SAMPLE

This sample provided a good $\overline{NPV}$ ($1.2505 \cdot 10^9$ \$) and $\overline{CO_2}^T$ ($6.8821 \cdot 10^5$ tonnes) balance. It converged after 137 iterations. Wind energy had a mean availability of 95%, which is coherent with the results of [18]. Figure 10 exhibits the histogram of the 137 NPV calculations, the NPV inverse cumulative distribution function (iCDF), and the P90-P50-P10 estimations[1]. Figure 11 depicts the cash flow of the iteration whose NPV estimation is the closest to $\overline{NPV}$. For this particular iteration, production occurred from year 2 to 21. In other words, 3 years less than the maximum expected lifetime of the field.

Table 3 reveals the sizes of the renewable components. In this table, SC and PC denote the storage and power capacities, respectively. The sample relies mostly on batteries to store and recover energy. This observation relates to the intended future research on hydrogen as a commodity rather than an electricity source. The high power capacity of the second electrolyzer does not seem optimal. For this reason, our future work includes optimizing the promising samples. By doing so, we intend to obtain solutions that further increase NPV and reduce CO_2 emissions.

[1] For clarification regarding P90, P50, and P10: if PX is equal to Y, it means that X% of the estimations are greater than or equal to Y.

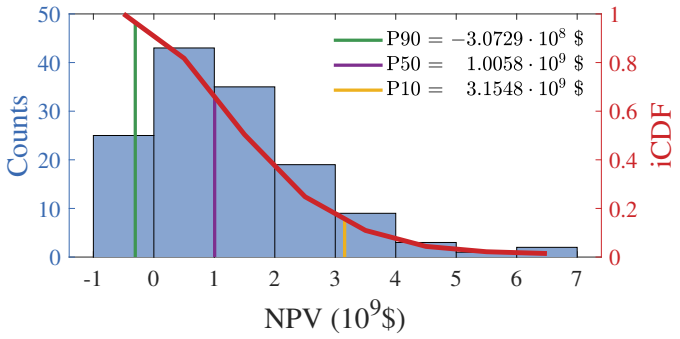

FIGURE 10: ECONOMIC RESULTS

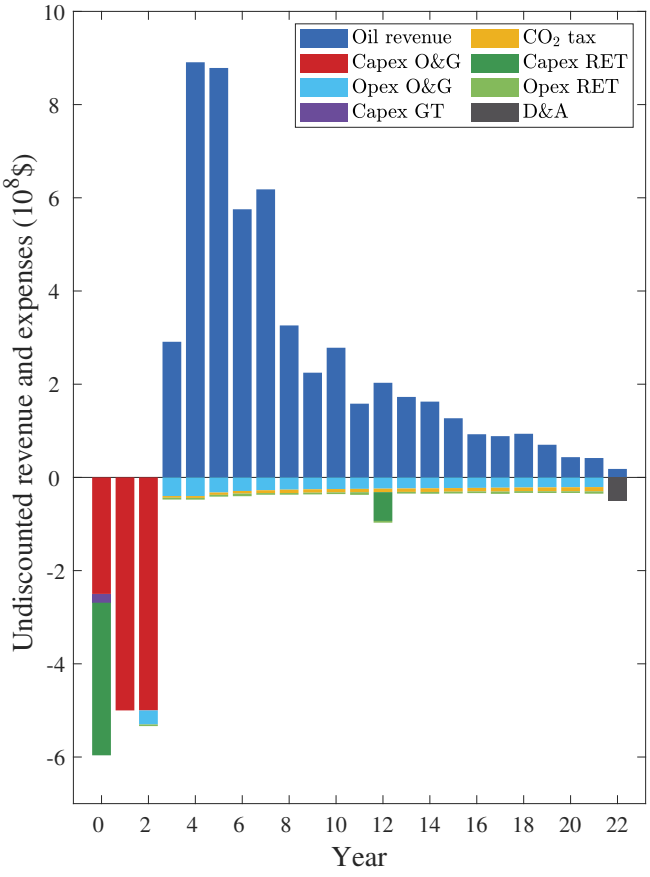

FIGURE 11: CASH FLOW

TABLE 3: SIZES OF THE RET COMPONENTS

RET	Value	RET	Value
WTs	7	PC fuel cell 1	2 MW
SC battery 1	169 MWh	PC fuel cell 2	1 MW
SC battery 2	186 MWh	PC electrolyzer 1	3 MW
PC battery 1	15 MW	PC electrolyzer 2	19 MW
PC battery 2	18 MW		